Systematic Investigations of the Influence of Molecular Structure on the Transport of Peptides Across Cultured Alveolar Cell Monolayers

A. N. O. Dodoo,[1] S. Bansal,[1] D. J. Barlow,[1,2] F. C. Bennet,[1] R. C. Hider,[1] A. B. Lansley,[1] M. J. Lawrence,[1] and C. Marriott[1]

Received September 17, 1999; accepted October 15, 1999

Purpose. To determine how the structures of peptides influence their alveolar permeability.
Methods. The studies were performed using 14 synthetic 'model' peptides, labelled with a novel, non-intrusive amino acid fluorophore, and their transport studied using rat alveolar cell monolayers cultured on permeable supports.
Results. The passage of the peptides across the epithelial cell monolayers is shown to be primarily paracellular, with an inverse dependence on molecular size, and an enhanced flux observed for cationic peptides. The apparent permeability coefficients (P_{app}) for the peptides (together with those for other organic solutes, taken from the literature) are shown to be well-modelled assuming two populations of 'pores' in the monolayers, modelled as cylindrical channels of radii 15 Å and 22 nm. The former pores are shown to be numerically equatable with the monolayer tri-junctional complexes, and the latter are taken as monolayer defects.
Conclusions. The various monolayer P_{app} values correlate well with the results from *in vivo* transport experiments, and the conclusion is drawn that the pulmonary delivery of peptide drugs is perfectly exploitable.

KEY WORDS: transport of peptides; molecular structure; molecular size; cultured alveolar cell monolayers; alveolar permeability.

INTRODUCTION

Over the last five years or so there have been many musings as to the potential to be afforded by using the pulmonary route of administration for the systemic delivery of protein and peptide drugs (1,2). There are no *systematic, comprehensive* studies yet reported, however, that demonstrate that the predicted potential is both real and achievable, although there have been several studies concerned with the alveolar permeability of specific peptides (cf., 3–5). In the following work we have endeavoured to rectify this deficiency, undertaking a systematic investigation of the alveolar cell permeability of 'model' peptides with defined physico-chemical characteristics.

In the design of the model peptides efforts were made to ensure that the compounds were chemically and metabolically stable, and had no propensity to form regular secondary structures. It was also deemed important to use peptides possessing a reasonable aqueous solubility and, as far as could be predicted, a lack of pharmacological activity.

[1] Department of Pharmacy, Franklin Wilkins Building, King's College London, 150 Stamford Street, London SE1 8WA, England.
[2] To whom correspondence should be addressed.

The three series of model peptides described in this study are based on the sequence triplet Gly-Ala-Ser and are presented in Table 1. Series I peptides were designed for the purpose of exploring the relation between alveolar absorption and peptide size. Series II peptides were designed with the aim of exploring the effects on alveolar absorption of modest (single residue) changes in hydrophobicity. Series III peptides were designed to permit an investigation of the influence of peptide charge on alveolar absorption.

To facilitate their preparation, detection and quantitation, all of the model peptides were synthesized incorporating the novel fluorescent amino acid *DL*-(6,7-dimethoxy-4-coumaryl) alanine (DCA, single letter code X*):

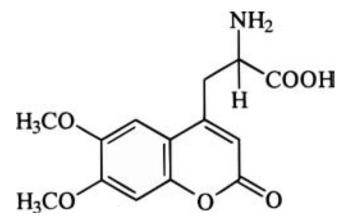

This label has previously been shown to be both chemically and metabolically stable, allowing the detection of peptides at concentrations as low as 5 picomolar (even in biological media), giving results identical with those obtained using radiolabelled species (6–7).

The transport properties of the model peptides were investigated using primary cultures of rat alveolar cells (nominally, type II cells), grown as monolayers on permeable supports.

MATERIALS AND METHODS

Peptide Syntheses

Peptide synthesis was carried out using Fmoc chemistry on a Perseptive Biosystems 9050 Pepsynthesizer. A PEG-polystyrene resin was used with a modified Rink amide linker. Fmoc amino acids were used in 4-fold excess and activation carried out using 2-(1H-benzotriazole-1-yl)-1,1,3,3-tetramethyluronium tetrafluoroborate in the presence of diisopropyl ethylamine. Peptides were cleaved from the resin using TFA, water and triisopropylsilane (95:4.5:0.5).

Synthesis of the Peptide Label

DL-(6,7-dimethoxy-4-coumaryl) alanine (DCA) was synthesized according to Bennett *et al.* (6–7). 3,4-dimethoxyphenol was condensed with ethyl-4-chloroacetoacetate in the presence of Amberlyst 15 to afford 4-chloromethyl-6,7-dimethoxycoumarin. Diethylacetamidomalonate was treated with sodium hydride followed by the 4-chloromethyl-6, 7-dimethoxycoumarin, and subsequent acid hydrolysis gave the novel amino acid, DCA.

Transport Studies

Alveolar cell monolayers were prepared according to Kim *et al.* (8). Alveolar cells were isolated from specific pathogen-free Sprague-Dawley male rats by digestion with porcine pancreatic elastase (2 U/ml; Worthington Biochemicals, NJ) and

0724-8741/00/0100-007$18.00/0 © 2000 Plenum Publishing Corporation

Table 1. Physicochemical and Transport Data for Model Peptides

	Peptide	*MW*	*r/Å*	*logP*	N_h	$P_{app} \times 10^7$/cm.s^{-1}
Series I	acX*$_{NH_2}$	334	4.5	−0.13 ± 0.01	12	1.88 ± 0.07 (n = 3) (AB)
						2.06 ± 0.09 (n = 3) (BA)
	acX*AS$_{NH_2}$	491	5.2	−1.25 ± 0.01	20	1.00 ± 0.27 (n = 17) (AB)
						1.04 ± 0.14 (n = 8) (BA)
	acX*ASGAS$_{NH_2}$	707	5.9	−2.51 ± 0.02	31	0.89 ± 0.19 (n = 4) (AB)
						0.65 ± 0.37 (n = 6) (BA)
	acX*AS(GAS)$_2$$_{NH_2}$	922	6.4	−3.43 ± 0.06	42	0.50 ± 0.24 (n = 6) (AB)
						0.69 ± 0.13 (n = 4) (BA)
	acX*AS(GAS)$_3$$_{NH_2}$	1137	6.9	−3.22 ± 0.03	53	0.60 ± 0.11 (n = 5) (AB)
	acX*AS(GAS)$_7$$_{NH_2}$	1998	8.3	−2.99 ± 0.05	97	0.41 ± 0.26 (n = 8) (AB)
						0.38 ± 0.11 (n = 3) (BA)
Series II	acX*AS$_{NH_2}$	491	5.2	−1.25 ± 0.01	20	1.00 ± 0.27 (n = 17) (AB)
						1.04 ± 0.14 (n = 8) (BA)
	acX*AV$_{NH_2}$	503	5.3	−0.13 ± 0.02	18	1.26 ± 0.27 (n = 4) (AB)
	acX*ASGAS$_{NH_2}$	707	5.9	−2.51 ± 0.02	31	0.89 ± 0.19 (n = 4) (AB)
						0.65 ± 0.37 (n = 6) (BA)
	acX*ASGAV$_{NH_2}$	719	6.0	−1.54 ± 0.03	29	0.98 ± 0.15 (n = 3) (AB)
	acX*AS(GAS)$_2$$_{NH_2}$	922	6.4	−3.43 ± 0.06	42	0.50 ± 0.24 (n = 6) (AB)
						0.69 ± 0.13 (n = 4) (BA)
	acX*AV(GAS)$_2$$_{NH_2}$	934	6.5	−2.76 ± 0.05	40	0.66 ± 0.03 (n = 3) (AB)
						0.59 ± 0.08 (n = 3) (BA)
Series III	acX*AS(GAS)$_2$$_{NH_2}$	922	6.4	−3.43 ± 0.06	42	0.50 ± 0.24 (n = 6) (AB)
						0.69 ± 0.13 (n = 4) (BA)
	X*AS(GAS)$_2$$_{NH_2}$	880	6.4	<−3.5	42	0.84 ± 0.04 (n = 4) (AB)
	acX*AS(GAS)$_2$	923	6.4	<−3.5	42	0.82 ± 0.16 (n = 8) (AB)
	acX*AS(GAD)$_2$$_{NH_2}$	978	6.5	<−3.5	46	0.48 ± 0.16 (n = 4) (AB)
	acX*ASGADGAK$_{NH_2}$	991	6.6	<−3.5	45	0.65 ± 0.35 (n = 6) (AB)
	acX*AS(GAK)$_2$$_{NH_2}$	1004	6.7	<−3.5	44	1.40 ± 0.31 (n = 3) (AB)

Note: Molecular weight (MW); molecular radius (r); log(octanol:water partition coefficient)(tabulated as logP, but for the series III peptides actually representing $\log D_{7.4}$); no. of potential hydrogen bonds formed with solvent water (N_h); apparent permeability coefficient for transport of the peptides across rat alveolar cell monolayers, in the apical-to-basolateral (AB) and basolateral-to-apical (BA) directions (values representing the mean ± standard deviation, calculated over n experiments). Amino acids shown using standard single letter code. X*, DL-(6,7-dimethoxy-4-coumaryl) alanine; ac, N-terminal acetyl group; NH_2, C-terminal amide group.

purified on discontinuous Percoll® gradients. The purified cells were cultured in a humidified atmosphere of 5% CO_2/95% air at 37°C, on tissue-culture treated polycarbonate filters (1.13 cm^2; Transwell®, Costar, MA), and seeded (day 0) at a density of 1.5×10^6 cells per cm^2. The cells were cultured in minimum essential medium supplemented with 10% v/v newborn bovine serum, 2 mM *L*-glutamate, 100 U/mL penicillin, 100 ng/mL streptomycin and 0.1 μM dexamethasone. The medium on both sides of the monolayer was changed on alternate days.

Transport experiments were carried out using a modified Ringer's solution (transport medium) comprising 1.8 mM $CaCl_2$, 0.81 mM $MgSO_4$, 5.4 mM KCl, 116.4 mM NaCl, 0.782 mM $NaH_2PO_4.2H_2O$, 5.55 mM *D*-glucose, 0.075 M bovine serum albumin (fraction V), 25 mM $NaHCO_3$ in 15 mM HEPES buffer pH 7.4. The cell monolayers were washed twice with transport medium and the apical and basolateral compartments filled with 0.6 mL and 1.5 mL transport medium, respectively. The cells were equilibrated with transport medium for 2 h at 37°C in a humidified 5% CO_2 incubator. Approximately 1 mM stock solutions of the model peptides were prepared in transport medium and trace amounts of ^{14}C-mannitol (DuPont Ltd, Herts, UK) added to each solution (to give a final activity of 0.5 μCi/mL). At the start of each transport experiment, half of the medium from the donor compartment was removed and replaced with an equal volume of peptide-containing medium, giving a final concentration of peptide in the donor medium of ~0.5 mM. At selected time intervals, 150 μL samples (for fluorescence assays) and 50 μL samples (for liquid scintillation counting) were taken from the receptor compartment and replaced with equal volumes of fresh transport medium. At the end of each transport experiment the donor and receptor compartment media were routinely assayed following separation by HPLC, to check for peptide breakdown products. Transepithelial resistance across the monolayers was monitored from day 2 using a Millicell® ERS system (Millicell, MA).

For all of the transport experiments performed, the integrity of the layers was routinely checked by monitoring their transepithelial electrical resistance (*TER*) and apparent permeability coefficient (P_{app}) for ^{14}C-mannitol.

Apparent permeability coefficients for the various solutes (P_{app}, in cm.s^{-1}) were calculated as:

$$P_{app} = (\Delta Q/\Delta t)/A \cdot c(0))$$

where $\Delta Q/\Delta t$ is the linear rate of appearance of solute in the receiver solution, A is the cross-sectional area of the polycarbonate filter (i.e., 1.13 cm^2) and $c(0)$ is the initial concentration of solute in the donor compartment at $t = 0$. The P_{app} values were not corrected for the P_{app} of the matrix-free filters (because this is at least 100-fold greater than the P_{app} for the matrix plus filter), nor were they corrected for aqueous boundary layer effects (since these are only significant for small non-electrolytes) (9).

The fluxes of the peptides across the alveolar cell monolayers were routinely determined in the apical to basolateral (AB) direction and, in most cases, also in the basolateral to apical (BA) direction, using an initial concentration of peptide in the donor chamber of 0.2 mM or 1 mM. Quantitation of the peptide flux was achieved by HPLC fluorescence monitoring of samples taken over a period of 4 h, using excitation and emission wavelengths of 345 nm and 445 nm, respectively (7).

Quantitation of Permeants

Liquid scintillation counting was used to determine ^{14}C mannitol levels in samples. 5 mL of Ready-Protein® scintillant was added to each 50 μL sample and radioactivity measured using a Rackbeta LKB 1209 Liquid scintillation counter (Rackbeta, Wallac, Turku, Finland).

Peptide concentrations were assayed following reversed phase HPLC separation, using a Kontron SFM-25 Fluorescence Spectrophotometer (Kontron Instruments, Zurich, Switzerland). The HPLC separations were obtained using a C_{18} analytical column (Vydac, Hesperia, CA) and Waters 60E systems controller with Waters 717 autosampler. The solvent systems employed for HPLC comprised solvent A: 0.1% v/v aq. TFA, and solvent B, 90% v/v acetonitrile + 10% v/v solvent A. The model peptides were resolved using 2 min elution with solvent A followed by a linear gradient of 10%–90% solvent B developed over 30 min at a flow rate of 1.5 mL per min.

Peptide Partitioning Experiments

Log P (and $logD_{7.4}$) determinations for the peptides were carried out at 25°C using *n*-octanol/Krebs Ringer buffer (pH 7.4), with each phase carefully equilibrated with the opposite phase before use. Peptide concentrations were determined by HPLC analysis (on a reversed phase C_{18} column using 0.1% TFA/acetonitrile gradients).

Modelling of the Peptide Permeability Data

The potential numbers of hydrogen bonds formed between the peptides and water (N_h) were calculated by summing the appropriate group contributions, taken as: $-OH$, 2; $-NH_2$, 2; $-C=O$, 2; $-NH_3^+$, 3; $-COO^-$, 4. Stokes radii of the peptides were calculated from their molecular volumes, obtained by summation of group volume increments taken from Chothia (10): Ala, 92 Å^3; Asp, 125 Å^3; Gly, 66 Å^3; Ser, 99 Å^3; Val, 142 Å^3; Lys, 171 Å^3. The molecular volume for DCA (390 Å^3) was calculated from density and MW data taken from the literature (11): coumarin, 260 Å^3; methoxy substituent on aromatic ring, 32 Å^3; peptide main chain (Gly), 66 Å^3.

Modelling of the alveolar cell monolayer P_{app} data was performed using eqs. (1) and (2), with the peptide molecular radii and calculated diffusion coefficients provided as input, and the sum of the squared differences between the calculated and observed P_{app} values minimised by iterative refinement of (ε/δ) and R, using a Hooke & Jeeves direct search optimisation routine, adapted from Bunday (12). For the series III peptides, the program input also included the peptide charge, and the value of $\Delta\Psi$ then refined with the values of ε/δ and R kept fixed.

RESULTS

The peptide transport data were acquired using only those monolayers with *TER* in the range 1050–1250 ohm.cm^2, so that their mean P_{app} for mannitol (which is taken to be the more sensitive indicator of their tight junctional integrity; ref 13) remained more or less constant (see Fig. 1), with a mean and 95% confidence limits of $2.14 \pm 0.66 \times 10^{-7}$ cm.s^{-1}. The consideration of such a restricted data set served to minimize the likelihood of significant inter-experiment variations in the monolayers employed, and so maximized confidence that meaningful comparisons could be made between the P_{app} for the different peptides tested.

Addressing first the issue of the mechanism of alveolar peptide transport, experiments were conducted to see how the rate of transport varied as a function of peptide concentration and the direction of passage across the monolayers. Since the AB fluxes for the smallest of the peptides ($_{ac}X^*NH_2$, and $_{ac}X^*ASNH_2$) vary in proportion with their concentration in the donor medium (cf., Fig. 2a), it is concluded that (at the concentrations tested) these two molecules do not pass across the monolayers by active transport. From this we also conclude that the same will hold true for the rest of the model peptides, simply because these are all much larger molecules. If the peptides were to cross the monolayers *via* some form of mediated transport mechanism, again we would expect (given the maximum size of substrate recognised by the known forms of peptide transporter; refs. 14–16) that the only molecules likely to exploit such a mechanism would be the capped amino acid $_{ac}X^*NH_2$, and the tripeptide, $_{ac}X^*ASNH_2$. We find, however, that (at the concentrations tested) the AB and BA fluxes for these peptides are identical within the limits of experimental error (Fig. 2b). We conclude, therefore, that either the two molecules move across the alveolar cells by passive diffusion, or else they undergo mediated transport exploiting transporters found in both the apical and basolateral membranes. Given the observed concentration dependence of the peptides' AB fluxes in a concentration range where the transporters are likely to be fully

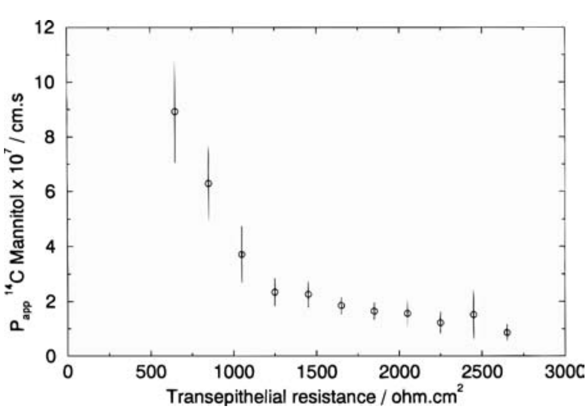

Fig. 1. Apparent permeability coefficient (P_{app}) for ^{14}C-mannitol in apical to basolateral transport across alveolar cell monolayers vs. the transepithelial electrical resistance (TER) of the monolayers. Data points represent the means and standard errors for P_{app} values calculated using monolayers with TER in intervals of 200 ohm.cm^2 from 650 ohm.cm^2 to 2650 ohm.cm^2.

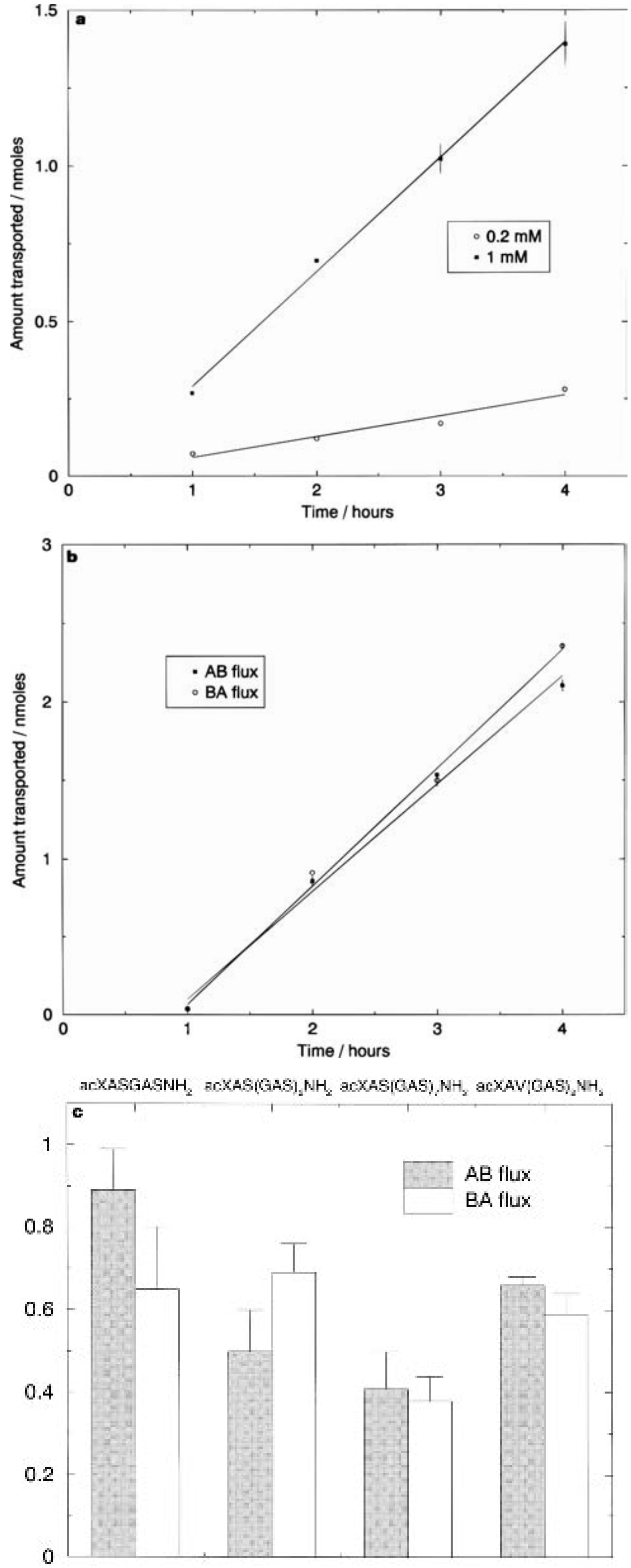

Fig. 2. (a) Concentration dependence of the AB flux of $acX{*}ASNH_2$ across alveolar cell monolayers (data represent the means of 3 determinations ± sem, error bars in some cases subsumed within symbol; legend shows initial concentrations of peptide). (b) Apical to basolateral (AB) and basolateral to apical (BA) flux of $acX{*}NH_2$ across alveolar cell monolayers (data represent the means of 3 determinations ± sem, error bars in some cases subsumed within symbol; initial peptide concentration, 0.78 mM). (c) Apparent permeability coefficients (P_{app}) for AB and BA fluxes of peptides across alveolar cell monolayers (data represent the means of ≥ 3 determinations ± sem).

saturated (14–16) (together with the difficulties in rationalising why peptide transporters would be needed on the basolateral side of alveloar epithelia) we conclude that the mechanism of transport of the peptides is most likely to involve passive diffusion. There are no statistically significant differences in the AB and BA P_{app} values for four of the larger peptides studied (as judged by two-tailed t-tests; Fig. 2c) and so all of the molecules are assumed to cross the alveolar cell monolayers in the same manner.

From the data obtained here, it is not possible to draw any unequivocal conclusions as to whether the peptides traverse the monolayers through the aqueous pores provided by the epithelial fight junctions (following the paracellular route) or whether they cross by diffusing through the cytoplasm of the cells, partitioning into and out of the apical and basolateral cell membranes (following the transcellular route). It seems highly probable, however, that their major route of passage is *via* the paracellular route. Such a conclusion is based on the combined observations that all of the peptides studied partition in favour of an aqueous medium rather than an organic/lipophilic medium (with negative *logP* values, Table 1) and have P_{app} that are consistently lower than the corresponding P_{app} measured for the hydrophilic solute, mannitol, which is widely recognised as a marker for the paracellular route (17).

With regard to peptide structure-permeability relationships, we find that the principal determinant of a peptide's flux across the alveolar epithelium is its size. In part this is demonstrated by the observation that the series I peptides show a generally inverse dependence of their AB P_{app} values on molecular weight (see Table 1), ranging from 1.88 (±0.07) × 10^{-7} cm.s^{-1} for $acX{*}NH_2$, down to 0.41 (±0.26) × 10^{-7} cm.s^{-1} for $acX{*}AS(GAS)_7NH_2$. Matsukawa *et al.* (18) have previously reported the same trend for a range of solutes transported across alveolar cell monolayers, and the same relationship has also been noted for transport of peptides across Caco-2 cell monolayers by Adson *et al.*(19). It must be noted here, however, that since the *logP* of the peptides in series I tend to decrease with increasing chain length, it is difficult to deconvolute completely the influences of their size and hydrophilicity. Our justification, therefore, for the conclusion that it is size, more so than hydrophilicity that governs alveolar peptide flux is provided by the observations made for series II peptides. With these three pairs of peptides a single Ser to Val substitution leads to a small *increase* in mass of 12, but causes a marked *decrease* in the peptide's hydrophilicity (that is, an increase in its *logP*; Table 1). Since the Ser to Val substitutions in all three lengths of peptides seem to result in insignificant differences in the peptide's AB P_{app}, it would thus appear that the change in size of the peptides in series I has more influence on transport rate than the change in *logP.*

If we err on the side of caution, however, and consider which physico-chemical property is most appropriate to guide in the task of peptide drug design, it is clearly best to try to predict alveolar permeability using an index that provides a combined measure of peptide size *and* hydrophilicity. For such

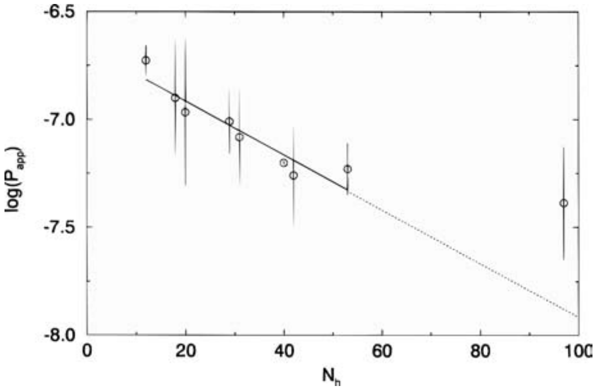

Fig. 3. log (P_{app}) vs. N_h for neutral 'model' peptides. The regression line shown (—) is calculated over the data for peptides with MW's < 1200, and the line then extrapolated beyond these data (····).

purposes we can use a simple count of the number of potential hydrogen bonds formed between the peptide and water (the parameter N_h listed in Table 1). This index has already found utility in analyses of solute transport into animal and plant cells (20), and also in more specific analyses of peptide transport across Caco-2 cell monolayers (21). If our assumption that peptides cross the alveolar epithelium by means of passive diffusion *via* the paracellular route is correct, then the use of N_h as a predictor of flux is, in any case, preferable to the use of *logP*. This is because *logP* provides a measure of the *relative* solubilities of the molecules in aqueous and organic media, which means that it is pertinent to the partitioning of drugs into and out of biological membranes, and is relevant therefore to the transcellular transport but not the paracellular transport of drugs. N_h, on the other hand is related much more directly to the aqueous solubility of a molecule and so will provide a relevant measure of the ability of a peptide to traverse the water-filled pores of the epithelial tight junctions. For any small linear peptide it is also likely to be related to the molecule's hydrodynamic diameter, and this too will have a bearing on the ease of passage of a peptide through the tight junctional pores.

Figure 3 shows the combined data for the 9 peptides in series I and II, with their $log(P_{app})$ values plotted against N_h. We see here that there is a log-linear dependence of P_{app} on N_h, for peptides with molecular weights less than ~1200. In the case of the one peptide studied that has a MW above this (acX*AS(GAS)$_7$NH$_2$; MW, 1998) there is some indication that its P_{app} is rather higher than would be predicted by this linear relation, and it may therefore be that large peptides such as this traverse the monolayer in a manner that is different from that exploited by the smaller molecules. Although it is difficult to determine precisely the nature of these transport routes, we show below that the data are best accounted for in terms of different populations of pores in the epithelial cell layer.

DISCUSSION

The mean effective radii of the tight junctional 'pores' (R) can be estimated from P_{app} data using the relation (22):

$$P_{app} = (\varepsilon/\delta)\cdot F(r|R)\cdot D \tag{1}$$

in which ε and δ are respectively the fractional cross-sectional area and mean path length of the pores, D is the diffusion coefficient of the transported solute, and $F(r|R)$ is the Renkin sieving function for cylindrical channels (23), obtained as:

$$F(r|R) = (1 - r|R)^2\,[1 - 2.104(r|R) + 2.09(r|R)^3 - 0.95(r|R)^5] \tag{2}$$

where r is the molecular radius of the solute.

Assuming a single population of uniformly-sized pores, and fitting to the AB P_{app} data obtained for the series I and II peptides, we obtain an effective pore radius of 22 Å, with the fractional area per unit length of these pores (ε/δ) calculated as 0.08 cm^{-1}. This model gives a respectable fit to the P_{app} data (Fig. 4a), but is deficient in several respects. It does not accord, for example, with the findings of Adson *et al.* (19), who used alveolar cell monolayers (of TER ~1200 ohm.cm^2) and (employing the same type of calculation) obtained a mean pore radius of 5.5 Å calculated from their P_{app} data for mannitol and urea. It also does not accord with the results reported by Matsukawa and co-workers (18), who used alveolar cell

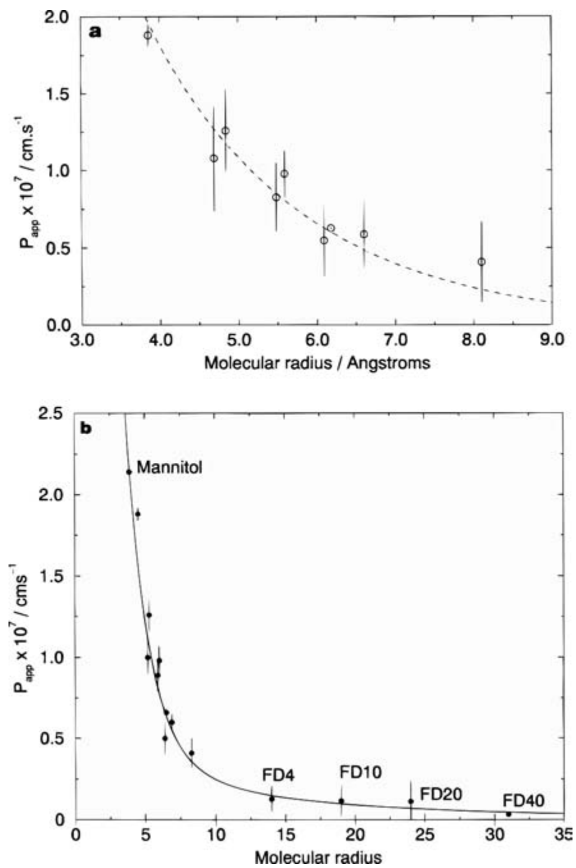

Fig. 4. (a) P_{app} vs. molecular radius for neutral 'model' peptides. The fitted curve is calculated assuming a single population of cylindrical 'pores' of radius of 22 Å. (b) Variation in monolayer P_{app} as a function of solute radius (in Å) with the experimental data plotted as filled circles and the solid line showing the calculated permeabilities assuming 2 populations of pores in the monolayers: cylindrical pores of radius 15 Å, and cylindrical pores of radius 22 nm. Transport data for fluoroscein isothiocyanate-labelled dextrans are taken from Matsukawa et al. (18) and their radii and diffusion coefficients calculated as: FD4, 14 Å, 1.75×10^{-6} cm^2.s^{-1}; FD10, 19 Å, 1.29×10^{-6} cm^2.s^{-1}; FD20, 24 Å, 1.02×10^{-6} cm^2.s^{-1}; FD40, 31 Å, 0.79×10^{-6} cm^2.s^{-1}.

monolayers (of mean TER, 2450 ohm.cm^2) to study the transport of a range of solutes including high molecular weight fluorophore-labelled dextrans and (again following a similar method of calculation) obtained a mean pore radius of 56 Å.

In view of these deficiencies, we elected to re-model the data, considering not just a single population of pores, but rather a mixture of two types of pores having differing radii and population sizes. The best-fitted values for the radii of such pores were obtained as 15 Å and 22 nm, with (ε/δ) of 0.089 cm^{-1} and 0.011 cm^{-1}, respectively.

This final two-pore modelling is eminently satisfying, and accounts for all of the available data remarkably well, with the fit between the measured and calculated P_{app} values (Fig. 4b) much improved over that shown by Matsukawa *et al.* (18). However, our estimated size for the smaller cylindrical pores (15 Å) is still somewhat larger than was estimated by Adson *et al.* (19), but this is because these authors considered only a single population of pores and used only the P_{app} data for two small solutes, mannitol and urea.

If we calculate the relative fluxes through the two different types of pores as a function of solute radius, we find that for molecules of the size of tripeptides (with r of ~5 Å) 40% of the transport is through the 22 nm pores, and 60% through the 15 Å pores. With hexapeptide-sized solutes (with r around 6 Å) the fluxes through the 15 Å and 22 nm pores are more or less equal.

As to the significance of these findings in regard to the morphology of the alveolar cell monolayers, it is important to note (as mentioned by Patton; ref 1) that pore size calculations of this sort, in truth only really provide a way of modelling the P_{app} data *mathematically,* and the 'pores' considered may not have any physical counterparts. However, if we equate δ with the span of the (typically, 3–5) tight junctional strands of the zona occludens (24), with each strand being composed of protein sub-units of mean diameter 8 nm (25), we obtain a value for δ in the range 25–40 nm. With this estimate for δ we can then use our calculated values for R and ε/δ to determine the densities of each type of pore in the monolayer. By this means we find that there are roughly 3.2 million 15 Å pores and 2.4 thousand 22 nm pores per cm^2. Now, given that the mean surface area of an alveolar (type II) cell is roughly 60 μm^2 (26), then there will be around 1.6 million cells per cm^2. The number of tri-junctional complexes will thus be roughly 3.2 million per cm^2 (i.e., an average of 1 junction per cell, assuming a hexagonal array of cells). We note, therefore, that our calculated dimensions and relative areas of the pores are consistent with a monolayer in which all cells are separated from their neighbours by tight junctions, with the 15 Å pores representing the tri-junctional complexes, and the 22 nm channels perhaps representing sparse holes or defects in the monolayers. (Alternatively, we might view the very large pore transport as the uptake of solutes *via* caveolae.)

Moving on to the series III peptides, to consider the effects of charge on alveolar peptide transport, we have that (22):

$$P^- = P^* \cdot (\kappa/e^{-\kappa} - 1) \tag{3}$$

for anionic species, and:

$$P^+ = P^* \cdot (\kappa/1 - e^{\kappa}) \tag{4}$$

for cationic species, where P^* is the permeability coefficient for size-restricted diffusion of the molecules (i.e., the permeability coefficient for the neutral image of the charged species) and κ is the dimensionless electrochemical energy function given as:

$$\kappa = e \cdot |z| \cdot \Delta\Psi/kT \tag{5}$$

where kT is the thermal energy, e is the unit charge of an ion, z is the number of charges borne on the cation or anion, and $\Delta\Psi$ is the electrochemical potential gradient.

Using the five anionic, cationic and zwitterionic peptides in series III, we computed their P^* values (using Eqs. (1–2), assuming the two pore model of the monolayer), and then using Eqs. (3–5), along with the charged peptides' P_{app} values, we obtained a best fit value for $\Delta\Psi$. The results of these various calculations are summarised in Table 2. The calculated value of $\Delta\Psi$ is 18.4 mV, which is entirely consistent with the value of 17.5 mV found for Caco-2 cell monolayers (19). Again like the Caco-2 cell monolayers, the alveolar cell monolayers appear to be cation selective (presumably because of the negatively-charged glycocalyx borne on the monolayers), with P^+/P^* being 1.41 for the singly charged X*AS(GAS)$_2$NH$_2$ and 1.94 for the doubly charged acX*AS(GA *D*-K)$_2$NH$_2$. For the anionic peptides, P^-/P^* is calculated as 0.69 for acX*AS(GAS)$_2$ and 0.45 for acX*AS(GA*D*-D)$_2$NH$_2$, whist the zwitterionic peptide, acX*AS(GA*D*-DGA*D*-K)NH$_2$, seems to be transported as a neutral molecule with $P^{\pm} \sim P^*$.

Finally, we may consider how these *in vitro* data correlate with our expectations for the permeabilities of peptides across the alveolar epithelia *in vivo*. We note first of all that our *in vitro* model of peptide transport is very similar to the model developed by Berg *et al.* (27). On the basis of their work with solute transport across isolated, perfused rat lungs, these authors showed that in the intact rat lung, the transport of a set of 11 hydrophilic solutes could be modelled assuming a mixture of two types of cylindrical pores/channels, of radii 5 Å and 34 Å, with the smaller pores accounting for roughly 99% of the total pore area. Since the solutes included in the *in vivo* experiments were all smaller than 6 Å radius, one cannot attach any great significance to the fact that there was no evidence found for a population of very large pores, and if in fact we calculate the mean radius of our small and large cylindrical pores, weighted in accordance with their relative areas, we obtain a 'single pore' size estimate of 38 Å, which is close to the value of 34 Å determined by Berg *et al.* (27).

As further support for our *in vitro* model of alveolar epithelial cell transport, we take our two-pore model of the alveolar cell monolayers and compare the calculated permeabilities (P_{calc}) for selected solutes with the experimentally-determined first order rate constants for the absorption of these same solutes across isolated, perfused rat lung (28). Plotting $log(k)$ against $log(P_{calc})$ (Fig. 5), we find an extremely good linear relation (with a correlation coefficient of 0.98), such that:

$$log(k) = 0.87(\pm 0.08)log(P_{app}) + 5.78(\pm\ 0.53) \tag{7}$$

Although this correlation is based on data for just seven different solutes, it is nevertheless encouraging given that the data are distributed fairly evenly along the fitted line, with the solutes considered having sizes covering one order of magnitude.

We conclude that the monolayers prepared as primary cultures of rat alveolar cells provide a reliable way of predicting the *in vivo* transport properties of solutes, and that peptides (as indeed any other class of compound) can be very effectively administered *via* the pulmonary route, even when they lie within

Table 2. Structural and Transport Data for the Series III Charged Peptides

Peptide	r/Å	z	$D \times 10^6$/ $cm^2.s^{-1}$	$P_{app} \times 10^8$ /$cm.s^{-1}$	$P^{\pm} \times 10^8$/ $cm.s^{-1}$	$P^* \times 10^8$/ $cm.s^{-1}$	$P^{\pm}/P^*$
$XAS(GAS)_2NH_2$	6.4	+1	3.82	0.84	0.96	0.68	1.41
$acXAS(GAS)_2$	6.4	−1	3.82	0.82	0.47	0.68	0.69
$acXAS(GAK)_2NH_2$	6.7	+2	3.67	1.40	1.20	0.62	1.94
$acXAS(GAD)_2NH_2$	6.5	−2	3.76	0.48	0.30	0.66	0.45
$acXASGADGAKNH_2$	6.6	±	3.71	0.65	0.64	0.64	1.00

Note: r, molecular radius; z, molecular charge; D, diffusion coefficient (calculated using the Stokes-Einstein equation); P_{app}, measured mean apparent permeability coefficient for transport of the peptide across rat alveolar cell monolayers; $P^{\pm}$, calculated permeability of the charged peptide; P*, calculated permeability for the neutral image of the peptide

the macromolecular size range. On the basis of the work reported here we consider that all peptides of more than three residues will cross the alveolar epithelium *via* the paracellular route; those with six residues or fewer passing through the tri-junctional complexes; and those that are larger mainly or wholly exploiting gaps/defects in the epithelium, or alternatively traversing the monolayer in caveolae. Given the general desire to develop peptide drugs involving six or fewer residues, the pulmonary route of administration would thus seem perfectly exploitable. Such molecules will be able to gain access to the systemic circulation through both the 15 Å and 22 nm pores. From the results reported here it would also seem that subtle changes in the hydrophobicity of peptides would probably not have too pronounced an affect on their alveolar permeability, and that if the molecules carried a net positive charge this would certainly enhance their permeability-with peptides incorporating imidazole groups (with pK_a's close to body pH) perhaps able to exploit both transcellular as well as paracellular routes for absorption.

ACKNOWLEDGMENTS

This work was funded through the MRC LINK Initiative with industrial contributions provided by Wellcome (now GlaxoWellcome), Ciba Geigy (now Novartis), ICI Pharmaceuticals (now Zeneca) and SmithKline Beecham.

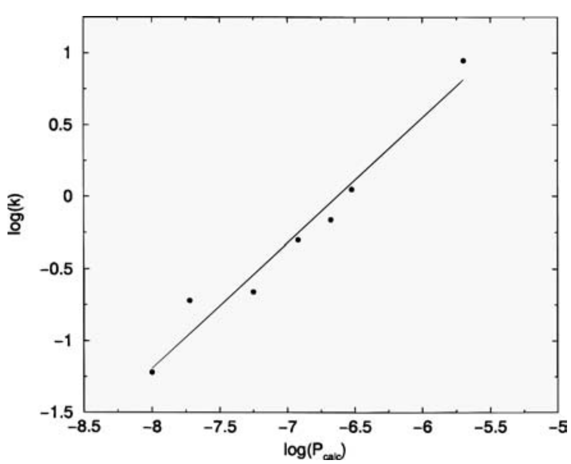

Fig. 5. Correlation between the calculated alveolar cell monolayer log(P_{app}) for selected solutes (P_{calc}, $cm.s^{-1}$) and their corresponding log(k) where k is the first order rate constant (in units of h^{-1}) for their absorption across isolated, perfused rat lungs. The data on k are taken from Schanker and Hemberger (28): urea (radius 2.7 Å), 8.85 h^{-1}; erythritol (radius 3.2 Å), 1.12 h^{-1}mannitol (radius 3.9 Å), 0.69 h^{-1}; sucrose (radius 5.6 Å), 0.50 h^{-1}; vitamin B_{12} (radius 7.0 Å), 0.22 h^{-1} inulin (radius 12.7 Å), 0.19 h^{-1}; FD20 (radius 24.0 Å), 0.06 h^{-1}.

REFERENCES

1. J. S. Patton, and R. M. Platz. Mechanisms of macromolecule absorption by the lungs, *Adv. Drug Del. Rev.* **19**:3–36 (1996).
2. D. A. Wall. Pulmonary absorption of peptides and proteins. *Drug Delivery* **2**:1–20 (1995).
3. L. Wang, D. Toledo-Velasquez, D. Schwegler-Berry, J. K. H. Ma, and Y. Rojanasakul. Transport and hydrolysis of enkephalins in cultured alveolar epithelial cell monolayers. *Pharm. Res.* **10**:1662–1667 (1993).
4. K. Morimoto, H. Yamahara, V. H. L. Lee, and K.-J. Kim. Dipeptide transport across alveolar epithelial cell monolayers. *Pharm. Res.* **10**:1668–1674 (1993).
5. H. Yamahara, K. Morimoto, V. H. L. Lee, and K.-J. Kim. Effects of protease inhibitors on vasopressin transport across rat alveolar epithelial cell monolayers. *Pharm. Res.* **11**:1617–1622 (1994).
6. F. M. Bennett, D. J. Barlow, A. N. O. Dodoo, R. C. Hider, A. B. Lansley, M. J. Lawrence, C. Marriott, and S. S. Bansal. L-(6,7-dimethoxy-4-coumaryl) alanine: an intrinsic probe for the labelling of peptides. *Tetrahedron Lett.* **38**:7449–7452 (1997).
7. F. M. Bennett, D. J. Barlow, A. N. O. Dodoo, R. C. Hider, A. B. Lansley, M. J. Lawrence, C. Marriott, and S.S. Bansal. Synthesis and properties of (6, 7-dimethoxy-4-coumaryl)alanine:a fluorescent peptide label. *Anal. Biochem.* **270**:15–23 (1999).
8. K.-J. Kim, D.-K. Suh, R. L. Lubman, S. I., Danto, Z. Borok, and E. D. Crandall. Studies on the mechanisms of action of active ion fluxes across alveolar cell monolayers. *J. Tiss. Cult. Meth.* **14**:187–194 (1992).
9. C. H. van Os, M. D. de Jong, and J. F. G. Slegers. Dimensions of polar pathways through rabbit gall bladder epithelium, *J. Membr. Biol.* **15**:363–382 (1974).
10. C. Chothia. Structural invariants in protein folding. *Nature* **254**:304–308 (1975).
11. R. C. Weast (ed)., *CRC Handbook of Chemistry & Physics*, CRC Press, Boca Raton Florida, 1987.
12. B. D. Bunday. *Basic Optimisation Methods*, Edward Arnold, Victoria, Australia, 1984.
13. P. Artusson, A.-L. Ungell, and J.-E. Löfroth. Selective permeability in two models of intestinal absorption: cultured monolayers of human intestinal epithelial cells and rat intestinal segments. *Pharm. Res.* **10**:1123–1129 (1993).
14. J. Bertran, A. Werner, G. Stange, D. Markovich, J. Biber, X. Testar, A. Zorzano, M. Palacin, and H. Murer. Expressions of Na^+ independent amino acid transport in Xenopus laevis oocytes by injection of rabbit kidney cortex mRNA. *Biochem. J.* **281**:717–723 (1992).
15. M. Boll, M. Herget, M. Wagener, W. M. Weber, D. Markovich, J. Biber, W. Clauss, H. Murer, and H. Daniel. Expression cloning and functional charaterization of the kidney cortex high-affinity proton-coupled peptide transporter. *Proc. Natl. Acad. Sci. (USA)* **93**:284–289 (1996).
16. Y.-J. Fei, Y. Kanai, S. Nussberger, V. Ganapathy, F. H. Leibach, M. F. Romero, S. K. Singh, W. F. Boron, and M.A. Hediger,

Expression cloning of a mammalian proton-coupled oligopeptide transporter. *Nature* **368**:563–566 (1994).
17. S. A. Lewis, J. R. Berg, and T. J. Kleine. Modulation of epithelial permeability by extracellular macromolecules. *Physiol. Rev.* **75**:561–589 (1995).
18. Y. Matsukawa, V. H. L. Lee, E. D. Crandall, and K.-J. Kim. Size-dependent dextran transport across rat alveolar epithelial cell monolayers. *J. Pharm. Sci.* **86**:305–309 (1997).
19. A. Adson, T. J. Raub, P. S. Burton, C. L. Barsuhn, A. R. Hilgers, K. L. Audus, and N. F. H. Ho. Quantitative approaches to delineate paracellular diffusion in cultured alveolar epithelial cell monolayers. *J. Pharm. Sci.* **83**:1529–1536 (1994).
20. W. D. Stein. *The movement of molecules across cell membranes*, Academic Press, New York, 1967.
21. R. A. Conradi, A. R. Hilgers, N. F. H. Ho, and P. S. Burton. The influence of peptide structure on transport across Caco-2 cells. *Pharm. Res.* **8**:1453–1460 (1991).
22. T. Teorell. In Butler, J. A. V. and Randall, J. T. (eds). *Progress in Biophysics and Biophysical Chemistry*, Academic Press, New York, Vol. 3, 1953, pp. 305–369.
23. F. E. Curry. In *Handbook of Physiology. The Cardiovascular System. Microcirculation*, Am. Physiol. Soc., Bethesda, MD, sect. 2, vol. IV, pt. 1, 1984, pp. 309–374.
24. P. Claude. Morphological factors influencing transepithelial permeability; a model for the resistance of the zonula occludens. *J. Membr. Biol.* **39**:219–232 (1978).
25. J. M. Anderson, M. S. Balda, and A. J. Fanning. The structure and function of tight junctions. *Curr. Opin Cell Biol.* **5**:772–778 (1993).
26. E. R. Weibel. In Fishman, A.P. and Fisher, A.B. (eds.), *Handbook of Physiology. The Respiratory System. Circulation & Non–respiratory functions*, Amer. Physiol. Soc., Bethseda, MA, sect. 3, vol. I, 1985, pp. 47–91.
27. M. M. Berg, K. J. Kim, R. L. Lubman, and E. D. Crandall. Hydrophilic solute transport across rat alveolar epithelium. *J. Appl. Physiol.* **66**:2320–2327 (1989).
28. L. S. Schanker and J. A. Hemberger. Relation between molecular weight and pulmonary absorption rate of lipid insoluble compounds in neonatal and adult rats. *Biochem. Pharmacol.* **32**:2599–2601 (1983).